Available online at www.sciencedirect.com
SCIENCE DIRECT®
Fusion Engineering and Design 65 (2003) 399–406
Fusion Engineering and Design
www.elsevier.com/locate/fusengdes

IFE chamber dry wall materials response to pulsed X-rays and ions at power-plant level fluences☆

T.J. Renk [a,*], C.L. Olson [a], T.J. Tanaka [a], M.A. Ulrickson [a], G.A. Rochau [a], R.R. Peterson [b], I.E. Golovkin [c], M.O. Thompson [d], T.R. Knowles [e], A.R. Raffray [f], M.S. Tillack [f]

[a] *Sandia National Laboratories, Albuquerque, NM, USA*
[b] *Los Alamos National Laboratory, Los Alamos, NM, USA*
[c] *Prism Computational Sciences, Madison, WI, USA*
[d] *Cornell University, Ithaca, NY, USA*
[e] *Energy Science Laboratories, Inc., San Diego, CA, USA*
[f] *University of California, San Diego, San Diego, CA, USA*

Abstract

We have begun a collaborative investigation of the response of candidate first-wall inertial fusion energy (IFE) reactor chamber drywall materials to X-rays on the Z facility, and to ions on RHEPP-1, both located at Sandia National Laboratories. Dose levels are comparable to those anticipated in future direct-drive reactors. Due to the 5–10 Hz repetition rate expected in such reactors, per-pulse effects such as material removal must be negligible. The primary wall materials investigated here are graphite and tungsten in various forms. After exposure on either RHEPP or Z, materials were analyzed for roughening and/or material removal (ablation) as a function of dose. Graphite is observed to undergo significant ablation/sublimation in response to ion exposure at the 3–4 J/cm^2 level, significantly below doses expected in future dry-wall power plants. Evidence of thermomechanical stresses resulting in material loss occurs for both graphite and tungsten, and is probably related to the pulsed nature of the energy delivery. These effects are not seen in typical magnetic fusion energy (MFE) conditions where these same kinds of materials are used. Results are presented for thresholds below which no roughening or ablation occurs. Use of graphite in a 'velvet' two-dimensional form may mitigate the effects seen with the flat material, and alloying tungsten with rhenium may reduce its roughening due to the increased ductility of the alloy.

Keywords: IFE chamber; Dry wall materials; X-ray

1. Introduction

The first-wall of an inertial fusion energy (IFE) power plant will be subjected to intense pulsed neutrons, X-rays, and energetic ions produced by the periodic explosion of a fusion pellet at the

☆ Sandia is a multiprogram laboratory operated by Sandia Corporation, a Lockheed–Martin Company, for the United States Department of Energy under Contract DE-AC04-94AL84000.

* Corresponding author.
E-mail address: tjrenk@sandia.gov (T.J. Renk).

0920-3796/03/$ - see front matter © 2003 Elsevier Science B.V. All rights reserved.
doi:10.1016/S0920-3796(03)00009-7

reactor center. Typical calculations for a direct-drive target (for yields of 150–400 MJ) with a dry wall at $r = 6.5$ m predict X-ray fluences of 0.3–1 J/cm^2 in a continuous spectrum peaked at several keV, and ion fluences of 8–20 J/cm^2, with ion energies into the MeV range. The X-rays will arrive at the wall first, within the first 20 ns, followed by a fast (fusion products) and slow (debris) ion pulse to the wall, lasting several microseconds. Neutron effects are beyond the scope of this paper. A collaborative program has been initiated to test IFE chamber wall materials response to X-rays on the Z facility, and to ions on RHEPP-1. Both Z and RHEPP-1 are located at Sandia National Laboratories. The Z machine typically uses a tungsten wire array Z-pinch target to produce X-ray fluences up to 3000 J/cm^2, in a continuous X-ray spectrum peaked at about 1 keV. The Z pulsewidth is about 8 ns, which is comparable to the timescale expected in future reactors. The RHEPP-1 (repetitive high-energy pulsed power) accelerator produces ion fluences up to 10 J/cm^2 per shot (for up to 1000 shots per sample), with ion energies as high as 1.5 MeV (for doubly charged particles). The ion arrival time is 200–300 ns, which is shorter than the debris ion arrival time, but comparable to the fusion product arrival time expected in future reactors. Accordingly, the dose thresholds discussed below may be somewhat conservative, that is, the thresholds may be slightly higher with the longer pulsewidths expected in fusion reactors.

Materials being considered for dry-wall designs with direct-drive are either flat monolithic (single material), composite armor/structural in nature, or textured materials such as velvet. At a repetition rate of 1 Hz, 3×10^7 pulses per year will impinge on the wall. To ensure survivability, almost no erosion of the flat wall surface per pulse can be tolerated (< 1 nm). Ions and photons of the energies and fluences discussed above will impinge normal to and penetrate well below the surface (1–10 μm), and can produce changes in near-surface microstructure and well as sublimation and ablation of the wall surface. In addition, it is known that roughening of the surface of alloyed materials can occur below ablation thresholds predicted for single-element materials, due to grain structure, entrained contaminant or alloying materials, second-phase particles from alloying, etc. For this study, we have several goals for materials to be tested for response to ion and X-ray doses on RHEPP and Z, respectively: (1) determine single-shot threshold for ablation, (2) characterize surface roughening occurring below this ablation threshold, (3) measure net ablation scaling for doses exceeding the ablation threshold and (4) determine if there is a dose threshold below which no effect occurs.

Leading candidate armor dry-wall materials include tungsten in either pure or alloy form, and graphite and/or carbon composites. Samples of these materials in flat geometry were prepared and exposed to both ions and X-rays in separate experiments, as detailed below. In addition, graphite in the form of 'velvet', i.e. long fibers oriented parallel to the flux direction was exposed to ion doses. Measurements of ablated material were made with 1- and 2-dimensional profilometry. Effects on surface topology and near-surface microstructure were studied using secondary electron microscopy (SEM) and ion induced secondary electron microscopy (IISEM). In the discussions below, these results are compared with predictions of materials response from the BUCKY [1] and SIM [2] modeling codes.

2. Experimental setup and procedures

Materials were exposed to ion beam doses were exposed on the repetitive high energy pulsed power (RHEPP-1) facility, which is described elsewhere [3,4]. The ion beam is formed in the magnetically confined anode plasma (MAP) ion diode. For this work, beams were formed from nitrogen (90% N/10% H) and CH_4 (70% C/30% H) injection. Energy deposition is similar for both beams. Diode voltage varied from 400 to 800 kV over the 100 ns power pulse, with the diode-sample distance typically 40 cm. Peak current densities were 150 A/cm^2 over a 100 cm^2 total area. The beam pulsewidth at the sample location increased to about 300 ns due to time-of-flight spreading. Nearby charge collectors monitored the ion beam fluence as a function of sample location. The ions

penetrate several microns into the test material, and induce a rapid heating, followed by rapid cooling (10^9 K/s) as the thermal pulse diffuses into the substrate. At high enough fluences, sublimation/ablation of the surface occurs.

For X-ray exposure, samples were fielded on the Z facility [5]. Due to the extreme conditions occurring during Z-pinch experiments, samples were mounted inside heavy stainless steel boxes, the front of which was located typically 50 cm from the wire array centerline. During and after the Z power pulse, there is the main X-ray burst, followed by debris from the wire array (stainless steel, copper, etc.). Finally, an overpressure wave deposits a layer of black soot on the samples. Debris from the filter is also deposited on the sample. Because of the low rate of experiments on Z, and because sample exposure was secondary to the main Z experiments, key goals for exposure were (1) maximizing of sample fielding rate per shot and (2) shielding of the sample surface from post X-ray debris. In addition, since the overall X-ray yield did not vary much from shot to shot, we achieved dose variation on samples by the use of polymer (Kimfol)/Al filters with an additional added Be foil. The Kimfol thickness was 2 μm, with a 1000 Å Al coating. Accordingly, on the front of each box fielded was a 1 cm aperture, followed by several baffle layers, a Kimfol/Al and Be filter (if included), and then the sample. The Be thicknesses used were 2.5 and 4.0 μm. Because of the added filtering, the peak of the photon spectrum shifted from about 300 eV in the unfiltered case to 1 keV with the Be filtering. Therefore, unlike the case with RHEPP-1 ion exposures, reduction in doses compared with non-filtered exposure was only achievable by hardening the X-ray spectrum, which of course changes the penetration depth of the photons impinging on the target. On RHEPP-1, dose reductions were achieved by increasing the radial position of the sample from the beam center, where peak beam power occurred. In addition, Z samples were exposed only once, compared with multiple ion exposures possible on RHEPP-1.

The aperturing/baffling greatly reduced the debris incident on the Z samples, but enough reached the sample surface to compromise attempts to measure changes in surface roughening from the (single) exposures. The typical wire array height was 2 cm, and at the sample location, a diameter of 0.8 cm was exposed to the X-ray pulse. This area was typically sectioned into 90° quadrants, so that four samples could be fielded per Z experiment. For a given shot, the X-ray dose at the sample location was determined from 3-dimensional view factor [6] simulations of the Z-pinch region. In these simulations, measured Z-pinch power and radius profiles are used as source inputs assuming a black-body emission spectrum. Time- and frequency-dependent flux on the sample surface was calculated by including albedo re-emission of all hardware within 15 cm of the Z-pinch.

3. Ion beam exposure experiments

The principal reactor dry-wall materials exposed to ions were (a) graphite and (b) tungsten. They will be discussed in turn.

3.1. Graphite

This has been a standard wall-facing material in magnetic fusion energy (MFE) research because of its high sublimation temperature, high thermal conductivity possible in certain formulations, and low atomic number. BUCKY modeling calculations were performed to predict graphite response to the RHEPP-1 ion beam, using the measured current density at the sample location, and propagated voltage based upon the corrected diode voltage. Thermal conductivity data characteristic of annealed pyrolitic graphite (PG) [7] was used. This form of graphite has very high conductivity compared with sintered graphite products such as Poco [8]. Three forms of graphite were treated-the PG, Poco, and 4-d carbon/composite weave. Mechanically polished samples were exposed to 75 pulses of the mixed C/H beam. Portions of each sample were shielded from the ion beam. The samples were then examined with linear profilometry, by scanning across the treatment interface. Fig. 1 shows the resultant ablation step heights as a function of beam dose for the 75 pulses. The BUCKY modeling prediction is also plotted. Note

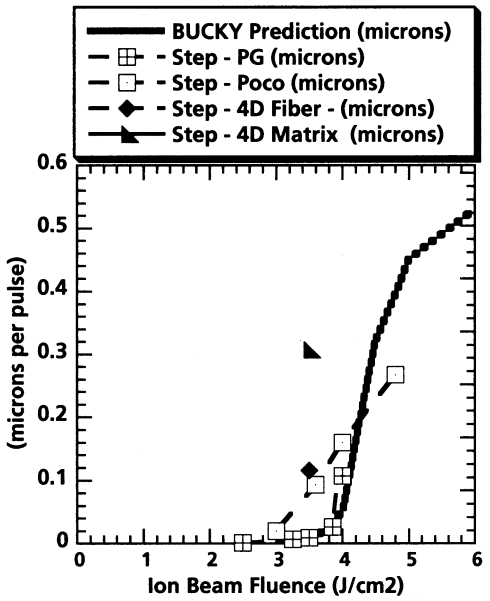

Fig. 1. Ablation response of various forms of graphite to 75 pulses of a 70% C/30% H ion beam. Ablation step was measured using 1-dimensional profilometry. Data from a BUCKY simulation are also included.

that (1) the PG ablation behavior follows closely the BUCKY curve, with an ablation threshold of between 3.5 and 4 J/cm^2; (2) the POCO exhibits a lower ablation threshold, followed by an ablation-with-dose increase that is less than that predicted by BUCKY; and (3) the 4-d weave ablates readily at 3.5 J/cm^2, with the fiber portion of the weave showing more resistance to ablation than the graphite matrix containing the fibers. A scan across the fibers indicated 9 μm ablation removal, whereas a similar scan across the matrix alone showed a 21 μm step height for material removed after 75 shots.

In any case, all forms of graphite are observed to readily ablate once a threshold dose is reached, and the amount of ablated material increases rapidly above this threshold. While the PG has a higher ablation threshold than the Poco, both show rapid per-pulse ablation at the 4 J/cm^2 dose level. This is to be compared with the 8–20 J/cm^2 ion dose to the first wall anticipated for future IFE reactor designs. The energy delivery time for those designs is expected to be longer than the pulse-width used in these experiments, which would increase the ablation threshold. But even if the 3.5 J/cm^2 threshold is substantially increased, the use of graphite in direct-drive IFE reactors can be considered to be problematic.

The roughening behavior of the graphite depended upon the graphite form. The Poco was observed to roughen at doses below 1 J/cm^2. Surface R_a measured by linear profilometry increased steadily as a function of dose from the 0.1–0.5 μm untreated values to as high as 3.5 μm at 4.8 J/cm^2. By contrast, the PG did not undergo any significant surface roughening, even when 8 μm was ablated away. Between 2.5 and 3.5 J/cm^2, some small amount of sublimation may be occurring with the PG, but not enough to be detectable by a 1-dimensional profilometer scan.

A possible alternative way to increase damage thresholds for a given IFE material is to consider a non-flat surface, i.e. a two- or even three-dimensional surface. An example of such an 'engineered' surface is a 'velvet' form of graphite. The graphite consists of straight, high-aspect ratio fibers oriented parallel to the flux direction. While the fiber tips may be eroded in the same way as uniformly flat graphite, the sides of the fibers effectively increase the surface area of the graphite by $\sim 50\times$. The ion dose to the fiber sides is greatly reduced, and the eroded fiber tip material can be expected to be redeposited in the interior of the fiber region, thus 'recycling' the graphite and perhaps extending its effective lifetime.

Such a 'velvet' was exposed to the RHEPP-1 beam in a similar manner to the graphites detailed above. The fibers were 2500 and 6.5 μm in length and width, respectively, with a packing fraction of 1.5%, i.e. only a small area of the Al backing material was covered with fiber shafts. The results of multiple ion beam exposure to the velvet are more qualitative in nature, because a way was not developed to measure any shortening of the fiber length due to ablation. Any fibers not oriented perpendicular to the backing surface were completely eroded. But (1) damage to the fiber side walls appeared slight, (2) the surface of the Al backing beneath the fibers, including some epoxy covering material, appeared undamaged after ion exposure, and (3) there was clear evidence of carbon redeposition at the base of the fibers.

3.2. Tungsten

A refractory metal, W is being increasingly used in MFE plasma-facing components. It is a very brittle metal, however, and this may affect its response to pulsed IFE discharges. The surface roughening threshold for W due to ions was measured with a laser reflectometer. A HeNe laser was propagated in situ to the sample surface through a fiber optic link. The reflected laser signal was transmitted by fiber optic to a photodiode detector. Any roughening of the W surface would be reflected in a reduced detector signal after the ion beam pulse. A 99.95% pure W flat sample with an initially mirror finish was exposed to an ion beam whose dose was increased in steps, starting at a relatively low level of 0.6 J/cm^2. The photodiode signal was monitored both pre- and post-pulse, and was observed to remain constant until a dose of 1.25 J/cm^2 was reached, over a total of over 40 pulses. At this level, each pulse then produced a progressive reduction in received signal from the previous pulse. Numerous cracks were visible on the treated W surface after treatment, and the linear R_a increased from 0.06 to 0.22 μm in the treated area. A SIM simulation of the W response to the 1.25 J/cm^2 energy input yielded a predicted maximum surface temperature of 1900 K. Since the melting point of W is 3680 K, we infer that the cracks are not caused by melt/solidification, but instead are probably caused by thermo-mechanical stress. That is, the heated near-surface layer is forced to expand and contract against the unheated W substrate, and the resulting strain cracks the surface.

W samples were exposed to higher ion beam doses, up to 6 J/cm^2. The surface roughening became much more pronounced. As a comparison, samples of a 75% W/25% Re alloy were also studied using the laser reflectometer. Re is added to increase the ductility of the alloy compared with the pure W. The roughening threshold increased to above 3 J/cm^2, compared with 1.25 J/cm^2 for the pure W. In addition, surface R_a was measured in both cases for beam doses up to 4 J/cm^2, and shown in Fig. 2. As can be seen, the W surface roughness increases steadily with dose to above 2.5 μm, whereas the R_a for the W/Re alloy remains

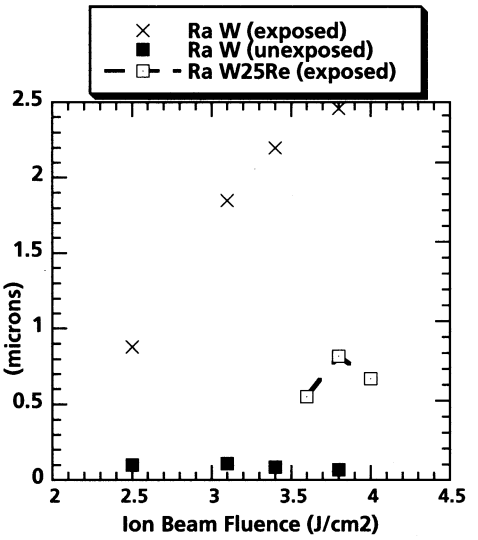

Fig. 2. Comparison of surface roughening (R_a) of W and W25Re samples exposed to 75 pulses of the C/H ion beam. Surface roughness was measured with 1-dimensional profilometry.

below 1 μm. This is presumably because of the higher ductility of the alloy. The W surface is characterized by raised ridges as much as 20 μm above the height in between the ridges, with surface cracks running along the tops of the ridges. Although both metals showed fine cracking, such large cracks were noticeably absent from the surface of the W/Re alloy.

4. X-ray exposure experiments

4.1. Graphite

A mechanically polished sample of Poco graphite was exposed on Z with the Kimfol/Al filter, but no added Be. The estimated dose was 8 J/cm^2. The sample was then sectioned and examined with SEM. A portion of the exposed and sectioned surface is shown in Fig. 3. The substrate appears at the bottom of the image, with a layer of debris on top, and an epoxy encapsulation. The debris appears bright in the SEM image because it consists of higher Z components. There was no ablation step indicated on this sample. The overall surface appears smooth under the debris, except

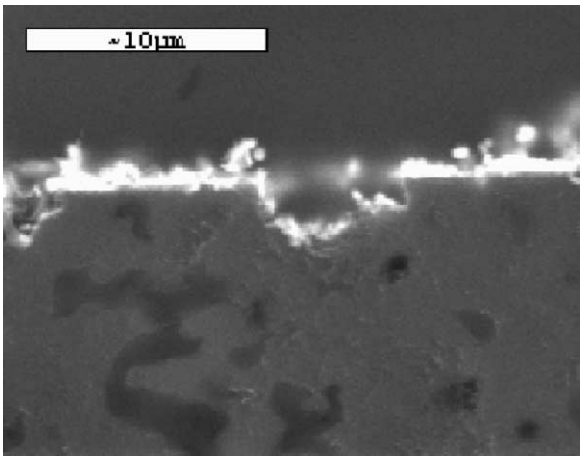

Fig. 3. SEM of a sectioned piece of Poco graphite after exposure to an estimated 8 J/cm^2 X-ray dose on Z. Although no ablation step is indicated, pieces of 2–5 μm size are missing from the surface after exposure.

for prominent pitted depressions of width ~ 5 μm, and extending a comparable distance below the surface. The pitting appears to be related to the grain size of the sintered graphite making up the Poco. It thus appears that thermomechanical stress, rather than sublimation, is the primary cause of the observed pitting.

4.2. Tungsten

Polished samples of 99.95% W and the W/Re alloy mentioned above were prepared and exposed in four similar wire array experiments. Each sample was thus exposed to the following dose levels: 19 J/cm^2 (unfiltered), 2.3, 1.3 and 1 J/cm^2. Two-dimensional surface profiles were constructed of each exposed sample to determine ablation step-height. Fig. 4 shows an area near the treatment interface for the pure W sample, exposed to 19 J/cm^2, which is illustrative of the analysis. The interface appears as a curved diagonal line from the lower left to upper right, with the treated area to the upper left. Note that (1) the treated area appears slightly darker then the untreated, and (2) there is more variation in the false-color image in the treated area, indicating more varied relief. (There is also debris in the treated area-in white). Overall, for this dose, a minimal ablation step is indicated, on the order of 0.2 μm or less. The W/Re alloy sample exposed at the same dose showed slightly less indication of removed material in the treated area, and less surface roughening. At doses below 2.3 J/cm^2, both sample sets showed little evidence of removed material and minimal roughening. The W/Re sample showed less evidence of roughening at 2.3 J/cm^2 compared with the pure W sample. At the 1 J/cm^2 exposure level (highest filter), there appears to be no effect on either the W or W25Re sample.

The treated W and W/Re samples were sectioned and studied with IISEM. Fig. 5 shows the sectioned W sample exposed to 19 J/cm^2 X-ray dose. The substrate appears as a network of false-color elongated grains in the horizontal direction, with vertically oriented (recrystallized) grains at the top, of about 2 μm thickness. (The curved line at the right-center of the sectioned image is a crater filled in by the light-colored Pt overcoating applied for the IISEM). The W appears to be melted to a depth of 2 μm. Such changes in grain structure have been associated with grain growth in metals subjected to elevated temperatures below their melting points [9]. Such conditions, however, occur over hundreds of seconds, whereas the sample in Fig. 5 was subjected to such temperatures for less than 1 μs. Note the clear demarcation line above which the grain change occurs. In view of these observations, it is almost certainly the case that the change in grain structure is caused by melting due to the X-ray exposure. A BUCKY simulation of this sample predicts a melt depth of only 0.8 μm, using the view factor simulation output as mentioned previously. The dose was scaled up to 60 J/cm^2, in an attempt to reproduce the 2 μm measured melt thickness. Over this range, the predicted melt depth remained unchanged, while the ablated thickness increased from 0.2 μm at 20 J/cm^2 to 0.5 μm at 60 J/cm^2. While the ablated thickness at 20 J/cm^2 is consistent with the measured sample, the inability of BUCKY to predict the 2 μm melt depth may be indicative of either a higher energy Z spectral distribution for $E > 3$ keV, or an improper treatment of the sample thermal conductivity. Accumulating data [10] from the Z machine suggests that such a high-energy component may exist, and could contain as much

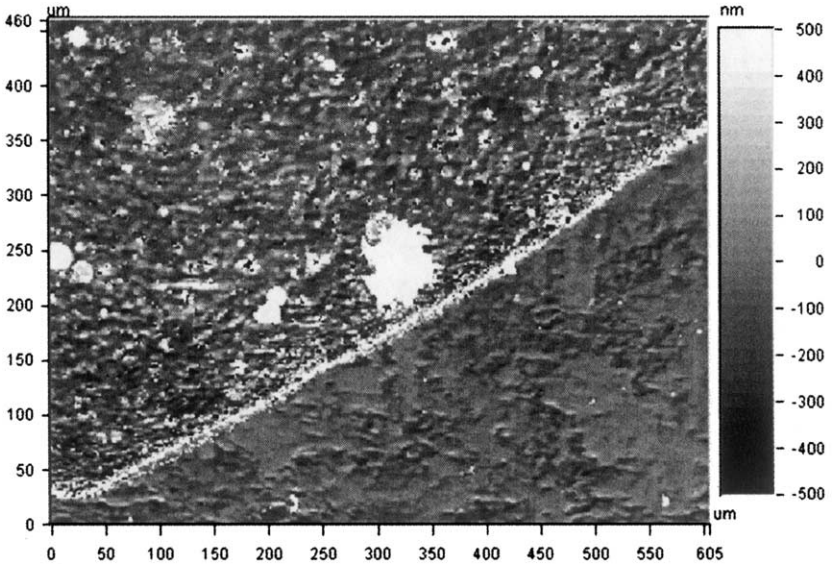

Fig. 4. False-color image of the interface area of a 99.95% W sample exposed to a 19 J/cm^2 X-ray dose on Z. The exposed area appears at upper left. There is a 0.2 μm ablation step indicated, with additional relief compared with the unexposed area (lower right).

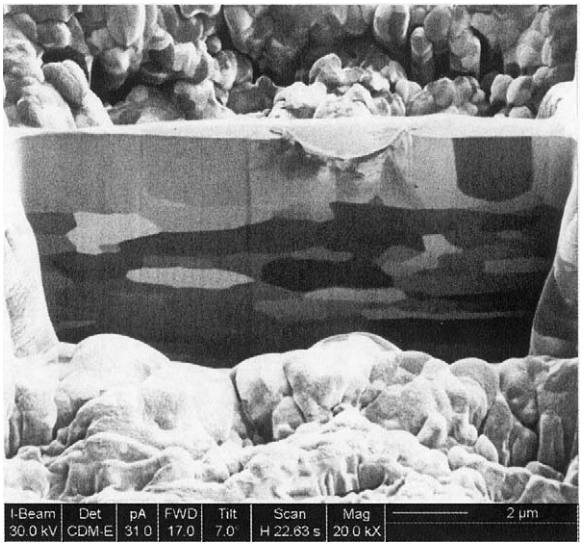

Fig. 5. Image from IISEM of a sectioned W sample exposed to a 19 J/cm^2 X-ray dose on Z. Unexposed grains appear in the middle of the image as flattened elongated shapes, above which is a lighter zone of recrystallized W about 2 μm thick.

as 10% of the total emitted X-ray power in the range $2 < E < 6$ keV. This would raise the predicted melt depth from BUCKY to more closely match the 2 micron This would also make the Z X-ray threat spectrum more nearly match that anticipated for future direct-drive IFE reactors.

5. Summary

Samples of graphite and tungsten were exposed to pulsed ions on RHEPP, and ions on Z. Dose levels and spectra are similar to those expected in future IFE direct-drive reactors. Graphite in all forms is observed to ablate readily at ion doses above 3.5 J/cm^2. Tungsten appears to exhibit thermomechanical roughening at doses lower than needed to melt the surface. Alloying with Re may reduce its tendency to roughen severely at higher doses. Poco graphite also appears to undergo thermomechanically-based material removal in response to 8 J/cm^2 X-ray dose on Z, even when no ablation step is indicated. Comparison with BUCKY Z simulations suggests the possibility of a higher-energy component to the Z spectrum than that inferred from an assumed black-body only spectrum.

Acknowledgements

Supported by NRL through the HAPL Program by the US Department of Energy, NNSA, DP.

References

[1] R.R. Peterson, D.A. Haynes, Jr, I.E. Golovkin, G.A. Moses, Inertial fusion energy target output and chamber response: calculations and experiments, Phys. Plasmas 9 (2002) 2287–2292.
[2] M.O. Thompson, T.J. Renk, Numerical modeling and experimental measurements of pulsed beam surface treatment, Mater. Res. Soc. Symp. Proc. 504 (1998) 33–38.
[3] H.C. Harjes, K.J. Penn, K.W. Reed, C.R. McClenahan, G.E. Laderach, R.W. Wavrik, J.L. Adcock, M.E. Butler, G.A. Mann, G.E. Pena, G.J. Weber, D. VanDeValde, L.E. Martinez, D. Muirhead, P.D. Kiekel, D.L. Johnson, E.L. Neau, Initial Results from the RHEPP module, in: D. Mosher, G. Cooperstein (Eds.), Ninth International Conference on High-Power Particle Beams (Beams 92), Washington, DC, NTIS PB92-206168, pp. 333–340.
[4] T.J. Renk, R.G. Buchheit, N.R. Sorensen, D.C. Senft, M.O. Thompson, K.S. Grabowski, Improvement of surface properties by modification and alloying with high-power ion beams, Phys. Plasmas 5 (1998) 2144–2150.
[5] R.B. Spielman, C. Deeney, G.A. Chandler, M.R. Douglas, D.L. Fehl, M.K. Matzen, D.H. McDaniel, T.J. Nash, J.L. Porter, T.W.L. Sanford, J.F. Seamen, W.A. Stygar, K.W. Struve, S.P. Breeze, J.S. McGurn, J.A. Torres, D.M. Zagar, T.L. Gilliland, D.O. Jobe, J.L. McKenney, R.C. Mock, M. Vargas, T. Wagoner, D.L. Peterson, Tungsten wire-array Z-pinch experiments at 200 TW and 2 MJ, Phys. Plasmas 5 (1998) 2105–2111.
[6] J.J. MacFarlane, J.E. Bailey, T.A. Mehlhorn, G.A. Chandler, T.J. Nash, C. Deeney, M.R. Douglas, Simulating the radiation environment in Z experiments using a 3D view factor code with 1D radiation-hydrodynamics emission modeling, Rev. Sci. Instrum. 72 (2001) 1228–1231.
[7] E.P. Roth, R.D. Watson, M. Moss, W.D. Drotning, Thermophysical Properties of Advanced Carbon Materials for Tokamak Limiters, Sandia National Laboratories, SAND88-2057, April 1989.
[8] Available from Poco Graphite Inc, Decatur, TX, USA.
[9] J. Almanslotter, M. Ruhle, Grain growth in Tungsten Wire, Int. J. Refract. Mets Hard Mets. 15 (1997) 295–300.
[10] M.E. Cuneo, Sandia National Laboratories, private conversation.